Nov 9th, 12:00 AM - 12:00 AM

Proposal for Codification of a DSM Design Approach for Cold-Formed Steel Short-to Intermediate Angle Columns

Pedro Borges Dinis

Dinar Camotim

Wei-Wen Yu International Specialty Conference on Cold-Formed Steel Structures
Baltimore, Maryland, U.S.A, November 9 & 10, 2016

Proposal for the Codification of a DSM Design Approach for Cold-Formed Steel Short-to-Intermediate Angle Columns

Pedro Borges Dinis[1] and Dinar Camotim[1]

Abstract

This paper presents a proposal for the codification of an efficient design approach for cold-formed steel short-to-intermediate equal-leg angle columns, consisting of a slight modification of a design approach developed by Dinis & Camotim (2015) and based on the Direct Strength Method (DSM). After (i) collecting the available experimental and numerical failure load data, comprising fixed-ended and pin-ended columns with several geometries (cross-section dimensions and length) and reported by various researchers, and (ii) briefly reviewing the mechanical reasoning behind the proposed procedures, the search for new/simpler expressions to provide the DSM design curves is addressed. Their merits are assessed through (i) the quality of the estimates of the available failure load data and (ii) the determination of the corresponding LRFD resistance factors. Concerning the latter, it is shown that the value recommended, for compression members, by the North American Specification (NAS) for the Design of Cold-Formed Steel Structural Members (AISI 2012), namely ϕ_c=0.85, can also be adopted for angle columns.

1. Introduction

In spite of their geometrical simplicity, angles exhibit a very complex structural behavior, which is responsible for the fact that the North American Specification (NAS) for the Design of Cold-Formed Steel Structural Members (AISI 2012) stipulates that short-to-intermediate equal-leg angle columns (i) are not yet pre-qualified for the design by means of the Direct Strength Method (DSM – Schafer 2008) and (ii) are excluded from the application of the Load and Resistance Factor Design (LFRD) resistance factor ϕ_c=0.85, valid for all other cold-formed steel compression members (Ganesan & Moen 2012). This is due to the fact that such columns buckle in flexural-torsional modes, associated with a practically horizontal P_{cr} vs. L curve "plateau", whereas their longer counterparts buckle in ("trivial") minor-axis flexural modes buckling – see the P_{cr} vs. L curves (L in logarithmic scale) plotted in Fig. 1 for fixed-ended (F) and pin-ended (P) angle columns.

[1] CERIS, ICIST, DECivil, Instituto Superior Técnico, Universidade de Lisboa, Av. Rovisco Pais, 1049-001 Lisboa, Portugal.

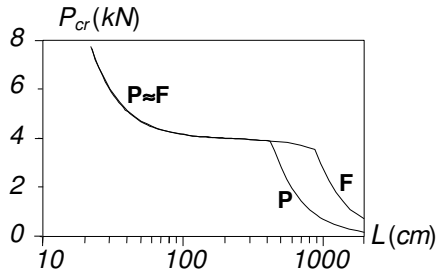

Fig. 1. P_{cr} vs. L curves for fixed-ended (F) and pin-ended (P) columns

Because the flexural-torsional buckling deformations in equal-leg angle columns are predominantly torsional and, therefore, akin (very similar) to local deformations, these columns have been said, erroneously, to fail in "local-global interactive modes", which explains why their design was often based on local strength concepts. Indeed, up to very recently, the most successful attempts to develop a DSM-based approach to design equal-leg angle columns, namely those reported by (i) Young (2004), for fixed-ended columns, (ii) Rasmussen (2006), for pin-ended columns[2], and (iii) Silvestre *et al*. (2013), for fixed and pin-ended columns, involved the use of either the currently codified DSM local design curve or a slightly modified (empirically) version of this curve. However, this situation was altered by the findings of Dinis *et al*. (2012) and Mesacasa *et al*. (2014), who provided clear numerical evidence that the failure of angle columns stems from the interaction between major-axis flexural torsional and minor-axis flexural buckling, a kind of unique coupling phenomenon that does not involve local deformations. Based on these findings, Dinis & Camotim (2015) proposed a rational DSM-based design approach for short-to-intermediate equal-leg angle columns that (i) uses genuine flexural-torsional strength curves (instead of the local one), (ii) is valid for both fixed-ended and pin-ended support conditions (it takes into to account effective centroid shift effects in pin-ended columns), and (iii) yields reliable predictions of the available experimental and numerical failure load data (ϕ_c=0.85 is applicable). However, a few improvements and simplifications, aimed at improving user-friendliness, are needed before this design approach may be deemed ready for codification.

The objective of this paper is to provide closure for this research effort, by proposing a DSM-based design approach for fixed-ended and pin-ended short-to-intermediate equal-leg angle columns that, in the authors' opinion, is ready for codification. It differs from the proposal of Dinis & Camotim (2015) in (i) the formulae providing four parameters appearing in the strength equations, which have been simplified, and (ii) the inclusion, in the merit assessment procedure, of the additional column experimental and numerical pin-ended column failure reported by Landesmann *et al.* (2016). After

[2] This designation stands for "cylindrically pinned" end supports – fixed with respect to major-axis bending and torsion (including fully restrained secondary warping), and pinned with respect to minor-axis bending.

presenting the collection of the available experimental and numerical failure loads, for both fixed-ended and pin-ended columns, the paper provides an overview of the main concepts and procedures involved in the DSM-based design approach proposed by Dinis & Camotim (2015). Then, the modification/simplifications incorporated in that design approach are addressed in detail, as well as their impact on the quality (accuracy and reliability) of the failure load predictions provided by the ensuing strength equations. In particular, the reliability assessment prescribed in AISI (2012) (see Section 1.1) shows that the LRFD resistance factors associated with the (modified) design approach proposed in this work never fall below ϕ_c=0.85.

1.1 Load and Resistance Factor Design (LRFD)

According to Section F.1.1 of the AISI (2012), the LFRD resistance factor ϕ_c is given by

$$\phi_c = C_\phi \left(M_m F_m P_m \right) e^{-\beta_0 \sqrt{V_M^2 + V_F^2 + C_P V_P^2 + V_Q^2}} \tag{1}$$

where (i) C_ϕ =1.52 (calibration coefficient for LRFD), (ii) M_m=1.10 and F_m=1.00 (taken from Table F1 of the specification) are the material and fabrication factor mean values, (iii) β_0 is the target reliability value (β_0=2.5 for structural members in LRFD), (iv) V_M=0.10, V_F=0.05 and V_Q=0.21 (again taken from Table F1 of the specification) are the material factor, fabrication factor and load effect coefficients of variation, respectively, and (v) C_p is a correction factor dependent on the number of tests. The P_m and V_p values are the mean and standard deviation of the "exact" (experimental and/or numerical)-to-predicted failure load ratios. The value recommended for compression members is ϕ_c=0.85, regardless of the column failure mode nature – but for short-to intermediate angle columns, which buckle in flexural-torsional modes, that value must be reduced.

2. Failure Load Data of Cold-Formed Steel Angle Columns

2.1 Experimental Failure Loads

The experimental failure loads already collected by Dinis & Camotim (2015) concern (i) 37 fixed-ended columns, tested by Popovic *et al.* (1999), Young (2004) and Mesacasa Jr. (2012), and (ii) 30 pin-ended columns, tested by Wilhoite *et al.* (1984), Popovic *et al.* (1999), Chodraui *et al.* (2006) and Maia *et al.* (2008)[3]. Those columns exhibit leg width (b), thickness (t) and length (L) values in the following ranges: 91.6 $mm \geq b \geq$ 50.0 mm, 4.7 $mm \geq t \geq$ 1.17 mm, 3500 $mm \geq L \geq$ 150 mm. Very recently, Landesmann *et al.* (2016) noted the lack of experimental failure loads of slender pin-ended columns and

[3] It is worth noting that 4 fixed-ended and 5 pined-ended columns tested by Popovic *et al.* (1999) were excluded from this investigation, due to the fact that thy did not buckle in flexural-torsional modes, *i.e.*, (their lengths are not located in the P_{cr} (L) curve plateau – they buckled in minor-axis flexural modes. Moreover, none of the 4 fixed-ended columns tested by Maia *et al.* (2008) was considered in the failure load database, since the ultimate strengths reported do not seem plausible – they are lower than those reported by the same authors for pin-ended columns with practically identical geometrical and material characteristics.

filled this gap carrying out a test campaign involving 20 such columns with cross-section dimensions and lengths t=1.55 *mm*, 90.0 $mm \geq b \geq$ 50.0 *mm*, 1200 $mm \geq L \geq$ 150 *mm*. Therefore, a total of 87 experimental failure loads are available (37 for fixed-ended columns and 50 for pin-ended columns), a number that may be deemed acceptable to assess the merits of the proposed DSM-based design approach for angle columns. The top part of Table 1 provides the numbers and origins of the available test results concerning fixed-ended and pin-ended angle columns – details on the measured specimen dimensions and steel properties can be found in the appropriate references.

Table 1. Available experimental and numerical failure loads test concerning fixed-ended and pin-ended equal-leg angle columns

	Fixed-ended columns		**Pin-ended columns**	
Experimental tests			Wilhoite *et al.* (1984)	8
	Popovic *et al.* (1999)	11	Popovic *et al.* (1999)	13
	Young (2004)	21	Chodraui *et al.* (2006)	4
	Mesacasa Jr. (2012)	5	Maia *et al.*(2008)	5
			Landesmann *et al.*(2016)	20
		37		50
Numerical simulations			Silvestre *et al.* (2013)	28
	Silvestre *et al.* (2013)	89	Dinis & Camotim (2015)	169
	Dinis & Camotim (2015)	248	Landesmann *et al.*(2016)	57
			This Work	42
Total		337		296

2.2 Numerical Failure Loads

Extensive parametric studies, consisting of ABAQUS (Simulia 2008) shell finite element analyses (SFEA), were conducted in the last few years to complement the experimental failure load data with numerical load data – the bottom part of Table 1 indicates the numbers and authorships of the available numerical results concerning fixed-ended and pin-ended angle columns. The modeling issues involved in the above studies can be found, for instance, in the work of Silvestre *et al.* (2013).

The numerical (SFEA) failure loads collected by Silvestre *et al.* (2013) and Dinis & Camotim (2015) and included in Table 1 concern 337 fixed-ended and 197 pin-ended columns, exhibiting (i) 7 cross-section dimensions (50×1.2*mm*, 50×2.6*mm*, 60×1.5*mm*, 70×1.2*mm,* 70×2.0*mm* and 90×2.5*mm*), (ii) lengths selected to ensure critical flexural-torsional modes buckling, *i.e.*, all columns located inside the P_{cr} vs. L curve "horizontal plateaus" (1200 $mm \geq L \geq$ 532 *mm*), and (iii) yield stresses chosen to cover a wide critical slenderness range: 1200 MPa $\geq f_y \geq$ 30 MPa[4]. Very recently, Landesmann *et al.* (2016)

[4] In order to achieve the above objective, it was necessary to consider several unrealistic (low and high) values.

carried out an additional set of 57 numerical simulations involving pin-ended columns with 5 cross-section dimensions (50×1.55*mm*, 60×1.55*mm*, 70×1.55*mm,* 80×1.55*mm,* 90×1.55*mm*), short-to-intermediate lengths (*i.e.*, buckling in flexural-torsional modes) and intermediate-to-high slenderness values – 600 MPa $\geq f_y \geq$ 250 MPa. Moreover, 42 pin-ended column failure loads, obtained from fresh numerical simulations carried out by the authors, are considered in this work, concerning angles with cross-section dimensions 110×5*mm*, lengths L = 950; 1000; 1500; 2000; 2500 *mm* and yield stresses in the range 1200 MPa $\geq f_y \geq$ 120 MPa. Therefore, a total of 633 numerical failure loads are available (337 for fixed-ended columns and 296 for pin-ended columns), a number providing a fairly extensive database for the merit assessment of the proposed DSM-based design approach for angle columns.

In all the numerical analyses, the steel material behavior was modeled as elastic-perfectly plastic and both residual stress and rounded corner effects were disregarded. Preliminary numerical studies showed that the combined influence of strain hardening, residual stresses and rounded corner effects has little impact on the angle column failure loads (differences never exceeding 3%), which is perfectly in line with the findings reported by other authors, namely Ellobody & Young (2005) and Shi *et al.* (2011).

The initial geometric imperfections considered in the numerical simulations take into account (i) the behavior observed in the experimental tests, namely the length-dependence of the imperfection-sensitivity, and (ii) the results of a detailed numerical investigation on the imperfection-sensitivity recently reported by Mesacasa Jr. *et al.* (2014), providing clear evidence about the relevance of the non-critical minor-axis flexural imperfection component (particularly in pin-ended columns). Indeed, although the columns with shorter lengths (located in left and central zones of the $P_{cr}(L)$ curve "horizontal plateaus") were found to be virtually insensitive to minor-axis flexural imperfections (only the critical flexural-torsional imperfections are relevant), it was decided to include, in all fixed-ended and pin-ended column numerical simulations, both flexural-torsional and minor-axis flexural initial geometrical imperfections. Concerning their amplitudes, they were equal to (i) 10% of the wall thickness t ($0.1\,t$), for the critical flexural-torsional components, and (ii) either $L/750$ (fixed-ended columns) or $L/1000$ (pin-ended columns), for the non-critical minor-axis flexural components – these values are in line with the measurements reported for the column specimens tested by Young (2004) (fixed-ended columns) and Popovic *et al.* (1999) (pin-ended columns). It is still worth mentioning that all the minor-axis flexural initial imperfection components were associated with initial mid-span major-axis translations "pointing" towards the cross-section corner – note that, in pin-ended columns, such initial imperfections are the most detrimental, since they reinforce the effective centroid shift effects (Young & Rasmussen, 1999)[5].

[5] Because of this "biased" minor-axis flexural initial imperfection components, it is logical to expect several pin-ended column experimental failure loads to be clearly underestimated by the proposed DSM-based design approach – a minor-axis flexural initial imperfection component "pointing" towards the cross-section leg free ends increases the column failure load (it opposes the effective centroid shift effects – Mesacasa Jr. *et al.* 2014).

3. Overview of the DSM Design Approach developed by Dinis & Camotim (2015)

Dinis & Camotim (2015) developed and validated a DSM-based approach for the design of thin-walled cold-formed steel fixed-ended and pin-ended equal-leg angle columns with short-to-intermediate lengths (*i.e.*, buckling in flexural-torsional modes) [6], hereafter termed "F columns" and "P columns", which was shown to provide accurate and reliable failure load predictions. The main features of this design approach are the following:

(i) It is based on the fact that most short-to-intermediate angle columns fail in interactive modes combing major-axis flexural-torsional and minor-axis flexural deformations.

(ii) It involves the use of (ii_1) the currently codified DSM global design curve and (ii_2) a set of genuine flexural-torsional strength curves (P_{nft}), developed in the context of columns with fully prevented minor-axis bending displacements. These strength curves, useful to design both F and P columns, make it possible to capture the progressive drop of the column post-critical strength as its length increases along the $P_{cr}(L)$ curve "horizontal plateau" – Figs. 2(a)-(c) show flexural-torsional strength curves concerning three columns with increasing lengths on the $P_{cr}(L)$ curve plateau.

(iii) The aforementioned effective centroid shift effects (Young & Rasmussen 1999), strongly affecting the pin-ended column failure loads (not the fixed-ended ones), are

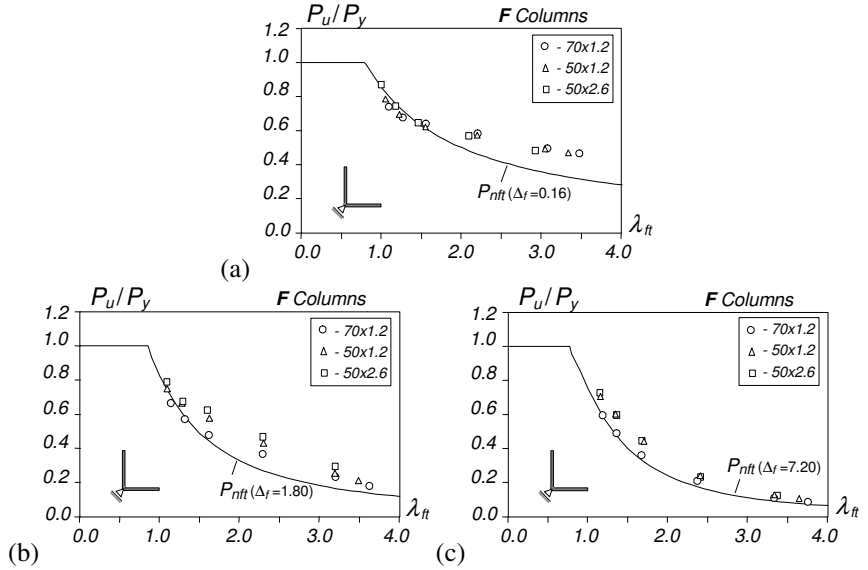

Fig. 2. Plots of P_u/P_y vs. λ_{ft} and proposed P_{nft} strength curves for fixed-ended columns with minor-axis bending displacements fully prevented and (a) Δ_f=0.16, (b) Δ_f=1.80 and (c) Δ_f=7.20

[6] The failure loads of the columns with longer lengths, which buckle in minor-axis flexural modes, are adequately predicted by the currently codified DSM global strength curve (AISI 2012).

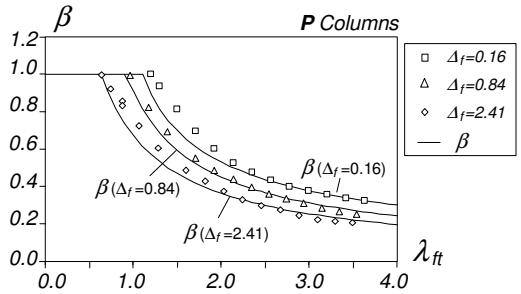

Fig. 3. Plots of the $\beta(\lambda_{ft})$ curves concerning pin-ended columns with Δ_f=0.16, 0.84 and 2.41

included in the design approach through a coefficient β, which must also reflect the change in column flexural-torsional post-buckling behavior along the $P_{cr}(L)$ curve plateau) – Fig. 3 displays the $\beta(\lambda_{ft})$ curves concerning three columns with increasing lengths on the $P_{cr}(L)$ curve plateau.

(iv) The length dependence of the column flexural-torsional post-critical strength and effective centroid shift effects is quantified by means of a parameter Δ_f, defined as

$$\Delta_f = \frac{f_{bt} - f_{crft}}{f_{bt}} \times 100 \tag{2}$$

where f_{bt} and f_{crft} are the pure torsional and major-axis flexural-torsional (critical) buckling stresses[7]. Such buckling stresses can be straightforwardly and exactly determined by means of the analytical expressions

$$f_{crft} = \frac{4}{5}\left(f_{bt} + f_{bf} - \sqrt{(f_{bt} + f_{bf})^2 - 2.5\, f_{bt}\, f_{bf}} \right) \tag{3a}$$

$$f_{bt} = G\frac{t^2}{b^2} + \pi^2 \frac{E\, t^2}{12(L/2)^2} \qquad f_{bf} = \pi^2 \frac{E\, b^2}{6(L/2)^2} \quad , \tag{3b}$$

where E and $G=E/[2(1+\nu)]$ are the steel Young's and shear moduli, and f_{bf} stands for the major-axis flexural buckling stress.

The end product of the research effort outlined in the above items are expressions of the strength curves providing the nominal strength, against the interactive failure under consideration (P_{nfte}), of fixed-ended and pin-ended angle columns, which are given by

---

[7] The use of parameter Δ_f is due to the fact that it was found that the length-dependence of the angle column structural response can be "measured" by the relative importance of major-axis flexure on the flexural-torsional buckling behavior (critical stress and buckling mode). Note that Eq. (2) differs slightly from the Δ_f definition originally put forward by Dinis & Camotim (2015) – f_{bt} appears in the denominator, instead of f_{crft}. This change was proposed by Landesmann *et al.* (2016), for the sake of rationality – these same authors showed that there is very little (negligible) impact on the quality of the failure load predictions.

$$P_{nfte}=\begin{cases}\beta\cdot P_{ne} & if \quad \lambda_{fte}\le\left(0.5+\sqrt{0.25-b}\right)\frac{1}{2a}\\ \beta\cdot P_{ne}\left(\frac{P_{crft}}{P_{ne}}\right)^{a}\left[1-b\left(\frac{P_{crft}}{P_{ne}}\right)^{a}\right] & if \quad \lambda_{fte}>\left(0.5+\sqrt{0.25-b}\right)\frac{1}{2a}\end{cases} \tag{4}$$

$$a=\begin{cases}0.001\,\Delta_f^3-0.032\,\Delta_f^2+0.25\,\Delta_f+0.4 & if \quad \Delta_f\le 5\\ 0.001\,\Delta_f+0.97 & if \quad \Delta_f>5\end{cases} \tag{5}$$

$$b=\begin{cases}0.014\,\Delta_f+0.15 & if \quad \Delta_f\le 7\\ 0.248 & if \quad \Delta_f>7\end{cases}, \tag{6}$$

where (i) parameter b should not be confused with the angle leg width, (ii) the values a=0.4 and b=0.15 were adopted for Δ_f=0, which amounts to saying that Eq. (4) coincides with the currently codified DSM local-global interactive strength curve for the shorter columns (f_{bt}/f_{crft} very close to 1), and (iii) the slenderness $\lambda_{fte}=(P_{ne}/P_{crft})^{0.5}$ is based on the column nominal strength against minor-axis flexural collapses (P_{ne}), obtained from the codified DSM global design curve

$$P_{ne}=\begin{cases}P_y\left(0.658^{\lambda_c^2}\right) & if \quad \lambda_c\le 1.5\\ P_y\left(\frac{0.877}{\lambda_c^2}\right) & if \quad \lambda_c>1.5\end{cases} \qquad \text{with} \quad \lambda_c=\sqrt{\frac{P_y}{P_{cre}}}, \tag{7}$$

where P_{cre} is the column minor-axis flexural buckling load and $P_y=Af_y$ is the squash load.

The coefficient β, which takes into account the effective centroid shift effects and follows an idea originally proposed by Rasmussen (2006), is obtained from

$$\beta=\begin{cases}1 & for\ F\ columns\\ \frac{0.68}{(\lambda_{fte}-c)^d}\le 1 & for\ P\ columns\end{cases} \tag{8}$$

$$c=\begin{cases}-300\,\Delta_f^3+110\Delta_f^2-12.8\Delta_f+1 & if \quad \Delta_f\le 0.2\\ -0.002\Delta_f^2-0.2\Delta_f+0.48 & if \quad 0.2<\Delta_f<5\\ 0.001\Delta_f-0.565 & if \quad \Delta_f\ge 5\end{cases} \tag{9}$$

$$d = \begin{cases} 380\ \Delta_f^3 - 140\,\Delta_f^2 + 15.2\,\Delta_f + 0.25 & \text{if} \quad \Delta_f \le 0.2 \\ -0.008\,\Delta_f^2 + 0.094\,\Delta_f + 0.712 & \text{if} \quad 0.2 < \Delta_f < 5 \\ 0.001\,\Delta_f + 0.977 & \text{if} \quad \Delta_f \ge 5 \end{cases} , \quad (10)$$

which amounts to saying that Eq. (8) coincides with Rasmussen's expression for the shorter columns (f_{bl}/f_{crfl} very close to 1), *i.e.*, one has c=1.0 and d=0.25 for Δ_f=0.

Finally, it is still worth mentioning that the expressions providing parameters a, b, c and d (Eqs. (5)-(6) and (9)-(10)) were obtained from "trial-and-error curve-fitting procedures", based on the numerical failure load data acquired by Dinis & Camotim (2015).

This DSM design approach provides quite accurate and reliable failure load predictions. Indeed, (i) Figs. 4(a)-(b) and 5(a)-(b) plot the P_u/P_{nfte} (failure-to-predicted) ratios against λ_{fte} (the average, standard deviation and maximum/minimum values of P_u/P_{nfte} are also given in those figures), and (ii) Table 2 shows the n, C_P, P_m, V_P and ϕ_c values (see Eq. (1)) obtained for the whole set of experimental and numerical column failure loads reported by Dinis & Camotim (2015) and obtained by Landesmann *et al.* (2016). The observation

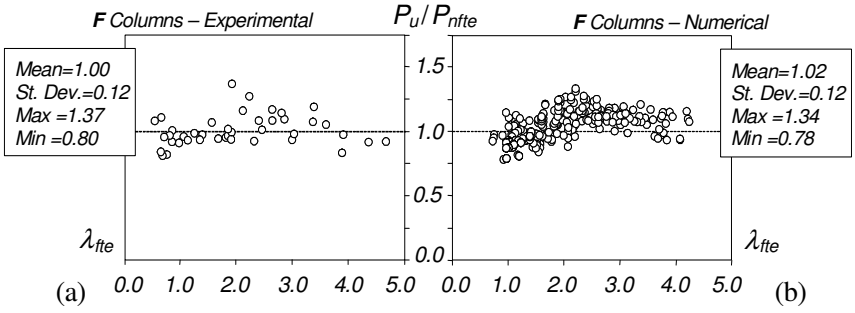

Fig. 4. Plots P_u/P_{nfte} vs. λ_{fte} for the F columns: (a) experimental and (b) numerical results

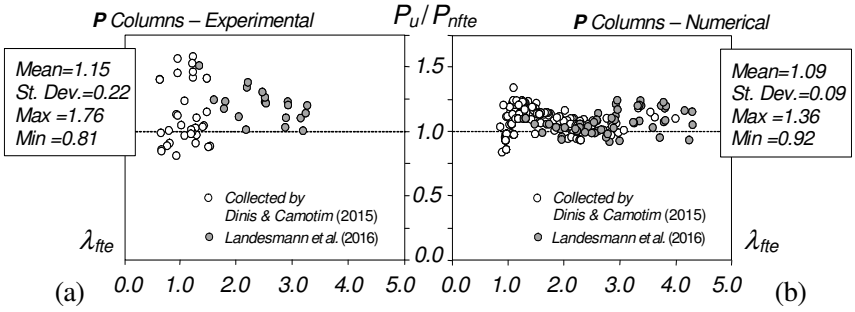

Fig. 5. Plots P_u/P_{nfte} vs. λ_{fte} for the P columns: (a) experimental and (b) numerical results

Table 2: LRFD ϕ_c values concerning the DSM prediction of the experimental, numerical and all failure loads reported in Dinis & Camotim (2015) and Landesmann *et al.* (2016)

DSM-F approach				DSM-P approach			
$\frac{P_u}{P_{nfte}}$	Exp	Num	Exp + Num	$\frac{P_u}{P_{nfte}}$	Exp	Num	Exp + Num
n	41	337	378	n	55	254	309
P_m	1.00	1.02	1.02	P_m	1.16	1.10	1.11
V_p	0.12	0.12	0.12	V_p	0.22	0.09	0.12
ϕ_c	0.85	0.88	0.88	ϕ_c	0.86	0.97	0.94

of these results clearly shows the quality of the performance indicators associated with the DSM design approach – most of all, it should be emphasized that the LRFD resistance factor ϕ_c=0.85 becomes applicable to cold-formed steel short-to-intermediate angle columns. Moreover, note that this design approach has the very important advantage of being rational, in the sense that it (i) reflects closely the angle column structural behavior and (ii) retains the current DSM global strength curve.

4. DSM Design Approach Proposed for Codification

Since it is felt that the expressions of the parameters a, c and d, given by Eqs. (5), (9) and (10), are a bit too complicated to be codified, it was decided to make an attempt to simplify them, without sacrificing the quality of the of the failure load predictions. Next, the simplification of the expressions providing parameters (i) a, associated with the flexural-torsional strength curves (see Eqs. (4)-(6)), and (ii) c and d, associated with the coefficient β (accounting for the effective centroid shift effects), are addressed separately.

4.1 Modification of the Flexural-Torsional Strength Curves – Parameter *a*

The search for a simpler expression for parameter a is based on the numerical failure load data reported by Dinis & Camotim (2015) and concerning fixed-ended columns with fully restrained minor-axis bending displacements, *i.e.*, "forced" to fail in a mode combining major-axis flexure and torsion. As before, the values a=0.4 and b=0.15 are adopted for Δ_f=0. The proposed new expression is a bi-linear approximation of Eq. (5) (note that Eq. (6), providing parameter b, is already bi-linear) and its coefficients were selected, by means of a "trial and error" procedure, to ensure flexural-torsional ultimate strength predictions as accurate as possible. It was found that the best approximation is

$$a = \begin{cases} 0.19\,\Delta_f + 0.4 & \text{if} \quad \Delta_f < 3 \\ 0.97 & \text{if} \quad \Delta_f \geq 3 \end{cases} \tag{11}$$

and Fig. 6 shows a comparison between the functions $a(\Delta_f)$ provided by Eqs. (5) and (11) – also shown is the (bi-linear) function $b(\Delta_f)$. Moreover, Figs 7(a)-(d) shows a comparison

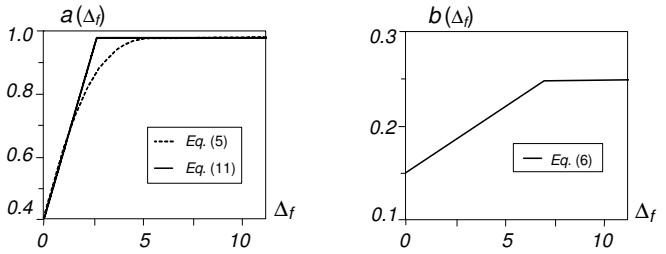

Fig. 6. Plots of parameters a and b against Δ_f

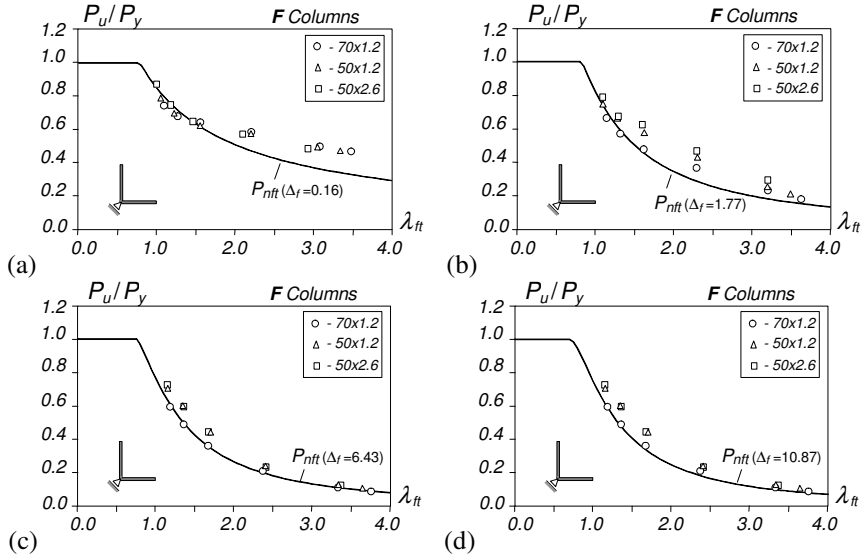

Fig. 7. Plots P_u/P_y vs. λ_{ft} and proposed P_{nft} strength curves for F columns with minor-axis bending displacements fully prevented, for (a) Δ_f=0.16, (b) Δ_f=1.77, (c) Δ_f=6.43 and (d) Δ_f=10.87

between the four flexural-torsional strength curves obtained with Eqs. (11) and (6), for Δ_f=0.16; 1.77; 6.43; 10.87, and the numerical failure loads that must be predicted by them. These figures clearly show that the P_{nft} values provide fairly accurate underestimations of the numerical failure loads – their quality is practically identical to that exhibited by the curves obtained with Eqs. (5) and (6), which were shown in Figs. 2(a)-(c).

It is worth noting that Eqs. (5) and (11) are valid only for Δ_f values up to 11.2. However, since a recent study on fixed-ended angle columns with stocky-to-moderate legs (Dinis *et al.* 2016) showed that, regardless of the cross-section geometry, Δ_f can never reach 11.2 (the flexural-torsional "horizontal plateau" never extends that far), the above $a(\Delta_f)$ bi-linear approximation is perfectly adequate.

In order to assess the impact of the $a(\Delta_f)$ function replacement, Figs. 8(a)-(b) plot P_u/P_{nfte} (failure-to-predicted load ratio) against λ_{fte} and show the corresponding averages, standard deviations and maximum/minimum values, for all the whole set of F column experimental and numerical failure loads considered in this work (see Section 2). Moreover, Table 3 gives the LRFD ϕ_c values obtained with the new $a(\Delta_f)$ expression. The comparison between Figs. 4 and 8, and Tables 2 (left part) and 3, makes it possible to conclude that the adoption of the new $a(\Delta_f)$ expression has virtually no impact on the DSM design approach indicators. Indeed, the averages, standard deviations, maximum values and minimum values of the experimental/numerical P_u/P_{nfte} ratios only vary by 0.00/–0.01, –0.01/–0.01, +0.03/–0.03 and +0.02/+0.00, respectively. Moreover, the ϕ_c values also remain practically the same (above 0.85): they increase by +0.01 for the experimental failure loads, and remain unchanged for the numerical and combined ones.

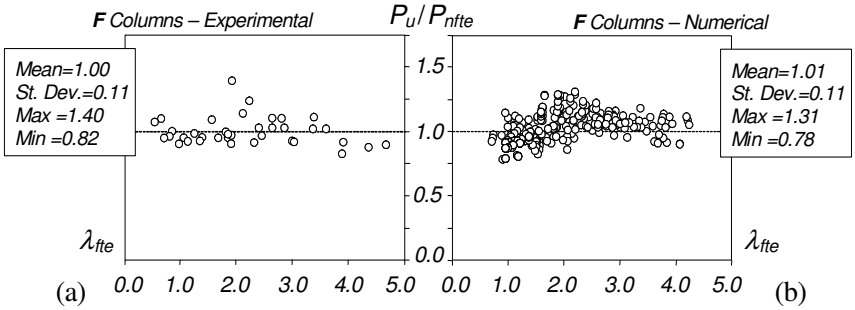

Fig. 8. Plots of P_u/P_{nfte} vs λ_{fte} for the F columns: (a) experimental and (b) numerical failure loads

Table 3: LRFD ϕ_c values concerning the DSM-F prediction of the experimental, numerical and combined failure loads

DSM-F procedure			
$\frac{P_u}{P_{nfte}}$	Exp	Num	Exp + Num
n	37	337	374
P_m	1.00	1.01	1.01
V_p	0.11	0.11	0.11
ϕ_c	0.86	0.88	0.88

4.2 Modification of the Reduction Coefficient β – Parameters c and d

Naturally, the search for simpler expression for parameters c and d is based on the elastic post-buckling results reported by Dinis & Camotim (2015) and concerning both fixed-ended and pin-ended columns. The proposed new expressions constitute now linear approximations of Eqs. (9) and (10) whose coefficients were selected, once more by means of a "trial and error" procedure, in order to capture, as accurately as possible, the

numerically determined strength erosion caused by the effective centroid shift effects. Moreover, it was decided to cease enforcing that c=1.0 and d=0.25 for Δ_f=0, a condition previously adopted for the sake of making Eq. (8) "compatible" with the expression proposed by Rasmussen (2006) for the very short columns ($\Delta_f \approx 0$). Note that adopting the above condition was not a very rational choice, since it led to functions $c(\Delta_f)$ and $d(\Delta_f)$ exhibiting rather non-linear and abrupt behaviors in the close vicinity of Δ_f=0 (see Fig. 9), a feature not at all confirmed by the numerical results. The best linear approximations were found to be

$$c = -0.2\ \Delta_f + 0.55 \tag{12}$$

$$d = 0.08\ \Delta_f + 0.72 \tag{13}$$

and Fig. 9 shows a comparison between these functions and those provided by Eqs. (9) and (10). Moreover, Fig. 10 compares, for Δ_f=0.16; 0.83; 2.35, the $\beta(\Delta_f)$ curves obtained with Eqs. (12) and (13) with the corresponding numerical β values reported by Dinis & Camotim (2015). These figures clearly show that these curves follow reasonably well the trends of the numerical result obtained, even if there are some perceptible differences – the most relevant ones concern the very slender shorter columns (Δ_f=0.16). Nevertheless, their estimation quality is practically identical to that exhibited by the previous curves, which have been presented in Fig. 3.

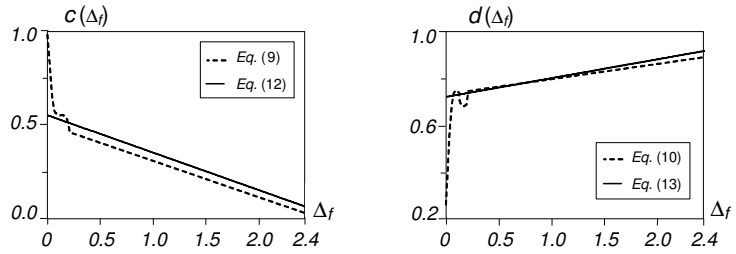

Fig. 9. Plots of parameters c and d against Δ_f

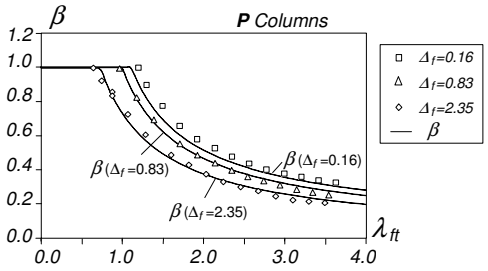

Fig. 10. Plots of the $\beta(\lambda_{ft})$ curves concerning P columns with Δ_f=0.16, 0.83, 2.35

It is worth that Eqs. (12) and (13) only need to be used for Δ_f values up to around 2.4. However, since a recent study on pin-ended angle columns with stocky-to-moderate legs (Dinis & Camotim 2016) showed that, regardless of the cross-section geometry, Δ_f never exceeds 2.43 (the flexural-torsional "horizontal plateau" of pin-ended angle columns never goes that far), the above $c(\Delta_f)$ and $d(\Delta_f)$ linear approximations are perfectly sound.

In order to assess the impact of the replacement of functions $c(\Delta_f)$ and $d(\Delta_f)$, Figs. 11(a)-(b) plot the P column P_u/P_{nfte} ratios against λ_{fte} and include the corresponding averages, standard deviations and maximum/minimum values, for all the whole set of P column experimental and numerical failure loads considered in this work (see again Section 2). Moreover, Table 4 gives the LRFD ϕ_c values obtained with the new $c(\Delta_f)$ and $d(\Delta_f)$ expressions. The comparison between Figs. 5 and 10, and Tables 2 (right part) and 4, makes it possible to conclude that the adoption of these expressions has also virtually no impact on the DSM design approach indicators. Indeed, the averages, standard deviations, maximum values and minimum values of the experimental/numerical P_u/P_{nfte} ratios only vary by –0.02/–0.05, –0.02/–0.01, –0.13/–0.09 and +0.02/–0.04, respectively – the most meaningful variations concern the maximum values and bring them down. Moreover, the ϕ_c values also remain practically the same (above 0.85): unchanged for the experimental failure loads and dropping by –0.04/–0.03 for the numerical/combined ones.

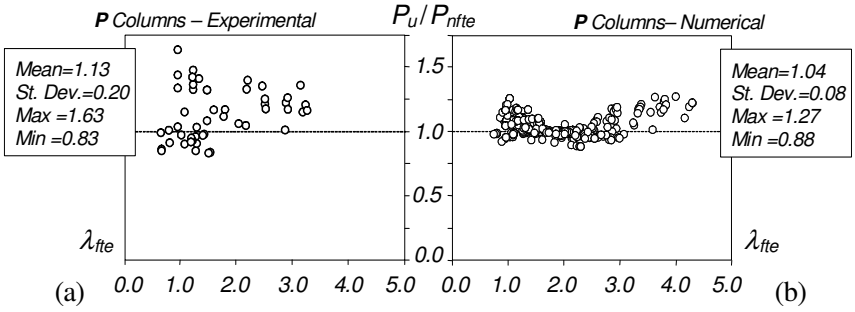

Fig. 11. Plots of P_u/P_{nfte} vs λ_{fte} for the P columns: (a) experimental and (b) numerical failure loads

Table 4: LRFD ϕ_c values concerning the DSM-P prediction of the experimental, numerical and combined failure loads

DSM-P procedure			
$\frac{P_u}{P_{nfte}}$	Exp	Num	Exp + Num
n	50	296	346
P_m	1.13	1.04	1.06
V_p	0.20	0.08	0.11
ϕ_c	0.86	0.93	0.91

4.3 Proposal

Taking into account the contents of the previous sections, it is the authors' belief that the DSM design approach for equal-leg fixed-ended and pin-ended equal-leg angle columns, defined by the expressions

$$P_{nfte} = \begin{cases} \beta \cdot P_{ne} & if \quad \lambda_{fte} \leq \left(0.5 + \sqrt{0.25 - b}\right)^{\frac{1}{2a}} \\ \beta \cdot P_{ne} \left(\frac{P_{crft}}{P_{ne}}\right)^{a} \left[1 - b \left(\frac{P_{crft}}{P_{ne}}\right)^{a}\right] & if \quad \lambda_{fte} > \left(0.5 + \sqrt{0.25 - b}\right)^{\frac{1}{2a}} \end{cases} \tag{14}$$

$$a = \begin{cases} 0.19\,\Delta_f + 0.4 & if \quad \Delta_f < 3 \\ 0.97 & if \quad \Delta_f \geq 3 \end{cases} \tag{15}$$

$$b = \begin{cases} 0.014\,\Delta_f + 0.15 & if \quad \Delta_f \leq 7 \\ 0.248 & if \quad \Delta_f > 7 \end{cases} \tag{16}$$

$$\beta = \begin{cases} 1 & for\ F\ columns \\ \dfrac{0.68}{(\lambda_{fte} - c)^{d}} \leq 1 & for\ P\ columns \end{cases} \tag{17}$$

$$c = -0.2\,\Delta_f + 0.55 \tag{18}$$

$$d = 0.08\,\Delta_f + 0.72 \tag{19}$$

can be readily proposed for codification, to be used with the LRFD resistance factor recommended for all other compression members (ϕ_c=0.85). Recall that one has (i) Δ_f=[(f_{bt}−f_{crft})/f_{bt}]×100, where f_{bt} and f_{crft} are obtained from Eqs. (3a)-(3b), and (ii) the slenderness λ_{fte}=(P_{ne}/P_{crft})$^{0.5}$ is used, where P_{ne} is obtained from the currently codified DSM global design curve.

5. Conclusion

This paper presented a proposal for the codification of an efficient DSM design approach for cold-formed steel equal-leg angle columns with short-to-intermediate lengths, *i.e.*, buckling in flexural-torsional modes. It consists of a modification/simplification of the design approach originally developed by Dinis & Camotim (2015) and slightly altered by Landesmann *et al.* (2016). Initially, the available experimental and numerical (shell

finite element) failure load data, concerning fixed-ended and pin-ended columns with several geometries (cross-section dimensions and length) and reported by various researchers, were collected and characterized. Next, a brief overview of the proposed DSM design approach was presented, including the mechanical reasoning behind the key concepts and procedures involved. Then, the main objectives of this work were addressed, namely (i) searching for new/simpler expressions to provide the DSM design curves and (ii) assessing the merits of those design curves through (ii_1) the quality of the prediction of the available failure load data and (ii_2) the determination of the corresponding LRFD resistance factors.

The search for the new/simpler expressions for the parameters a, c and d, appearing in the originally proposed DSM design approach (see Eqs. (4)-(10)) was successful and led to either bi-linear (a) or linear (c and d) functions of Δ_f, which replaced the original cubic or quadratic or ones – b was already provided by a bi-linear function. The impact of replacing the above three functions, on the quality (accuracy and reliability) of the failure load predictions provided by the ensuing strength equations, was then addressed in detail. It was found that such impact is minute (negligible), since the indicators of the exact-to-predicted failure load ratios provided by the DSM design approach based on the new functions $a(\Delta_f)$, $c(\Delta_f)$ and $d(\Delta_f)$ remain practically unaltered (some even improve). In particular, it was shown that the value recommended, for compression members, by the North American Specification for the Design of Cold-Formed Steel Structural Members (AISI 2012), namely ϕ_c=0.85, can also be adopted for angle columns. Indeed, the three ϕ_c values obtained on the basis of the experimental, numerical and combined experimental-numerical failure loads were all higher than 0.85. Therefore, it seems fair to argue that the proposed DSM design approach, defined by Eqs. (14)-(19) is ready for codification.

References

AISI (American Iron and Steel Institute) (2012). *North American Specification* (NAS) *for the Design of Cold-Formed Steel Structural Members* (AISI-S100-12), Washington DC.

Chodraui GMB, Shifferaw Y, Malite M and Schafer BW (2006). Cold-formed steel angles under axial compression, *Proceedings of 18th International Specialty Conference on Cold-Formed Steel Structures* (Orlando, 26-27/10), R. LaBoube, W.W. Yu (eds.), 285-300.

Dinis PB and Camotim D (2015). A novel DSM-based approach for the rational design of fixed-ended and pin-ended short-to-intermediate thin-walled angle columns, *Thin-Walled Structures*, **87**(February), 158-182, 2015.

Dinis PB and Camotim D (2016). Behavior and design of hot-rolled steel pin-ended short-to-intermediate columns, *Proceedings of 7th International Conference on Coupled Instabilities in Metal Structures* (CIMS 2016 – Baltimore, 7-8/11), accepted for publication.

Dinis PB, Camotim D and Silvestre N (2012). On the mechanics of angle column instability, *Thin-Walled Structures*, **52**(March), 80-89.

Dinis PB, Camotim D and Preto V (2016). Behaviour and design of short-to-intermediate hot-rolled steel angle columns, *Proceedings of International Colloquium on Stability and Ductility of Steel Structures* (SDSS 2016 – Timisoara, 30-5/1-6), in press.

Ellobody E and Young B (2005). Behavior of cold-formed steel plain angle columns, *Journal of Structural Engineering* (ASCE), **131**(3), 469-478.

Ganesan K and Moen CD (2012). LRFD resistance factor for cold-formed steel compression members, *Journal of Constructional Steel Research*, **72**(May), 261-266.

Landesmann A, Camotim D, Dinis PB and Cruz R. (2016). Short-to-intermediate slender pin-ended cold-formed steel equal-leg angle columns: experimental investigation, numerical simulation and DSM design, *submitted for publication*.

Maia WF, Neto JM and Malite M (2008). Stability of cold-formed steel simple and lipped angles under compression, *Proceedings of 19th International Specialty Conference on Cold-Formed Steel Structures* (St. Louis, 26-27/10), R. LaBoube, W.W. Yu (eds.), 111-125.

Mesacasa Jr. E (2012). *Structural Behavior and Design of Cold-Formed Steel Angle Columns*, MASc Thesis in Structural Engineering, School of Engineering at São Carlos, University of São Paulo, Brazil. (Portuguese)

Mesacasa Jr. E, Dinis PB, Camotim D and Malite M (2014). Mode interaction and imperfection-sensitivity in thin-walled equal-leg angle columns, *Thin-Walled Structures*, **81**(August), 138-149.

Popovic D, Hancock GJ and Rasmussen KJR (1999). Axial compression tests of cold-formed angles, *Journal of Structural Engineering* (ASCE), **125**(5), 515-523.

Rasmussen KJR (2006). Design of slender angle section beam-columns by the direct strength method, *Journal of Structural Engineering* (ASCE), **132**(2), 204-211.

Schafer BW (2008). Review: the direct strength method of cold-formed steel member design, *Journal of Constructional Steel Research*, **64**(7-8), 766-778.

Shi G, Liu Z, Ban HY, Zhang Y, Shi YJ and Wang YQ (2011). Tests and finite element analysis on the local buckling of 420 MPa steel equal angle columns under axial compression, *Steel and Composite Structures*, **12**(1), 31-51.

Silvestre N, Dinis PB and Camotim D (2013). Developments on the design of cold-formed steel angles, *Journal of Structural Engineering* (ASCE), **139**(5), 680-694.

Simulia Inc. (2008). *Abaqus Standard* (vrs. 6.7-5).

Wilhoite GM, Zandonini R and Zavelani A (1984). Behaviour and strength of angles in compression: an experimental investigation, *Proceedings of ASCE Annual Convention and Structures Congress* (San Francisco, 1-3/10).

Young B (2004). Tests and design of fixed-ended cold-formed steel plain angle columns, *Journal of Structural Engineering* (ASCE), **130**(12), 1931-1940.

Young B and Rasmussen KJR (1999). Shift of effective centroid in channel columns, *Journal of Structural Engineering* (ASCE), **125**(5), 524-531.